

Localization of polymers in a finite medium with fixed random obstacles

Y.Y. Goldschmidt^a and Y. Shiferaw

Department of Physics and Astronomy, University of Pittsburgh, Pittsburgh PA 15260, USA

Received 14 August 2001

Abstract. In this paper we investigate the conformation statistics of a Gaussian chain embedded in a medium of finite size, in the presence of quenched random obstacles. The similarities and differences between the case of random obstacles and the case of a Gaussian random potential are elucidated. The connection with the density of states of electrons in a metal with random repulsive impurities of finite range is discussed. We also interpret the results obtained in some previous numerical simulations.

PACS. 36.20.Ey Conformation (statistics and dynamics) – 05.40.-a Fluctuation phenomena, random processes, noise, and Brownian motion – 75.10.Nr Spin-glass and other random models – 64.60.Cn Order-disorder transformations; statistical mechanics of model systems

1 Introduction

The behavior of polymer chains in random media is a well studied problem both theoretically [1–8] and experimentally [9–12] and has applications in diverse fields. For polymers, the interest arises when the chains are confined inside an intertwined gel network [12], and perhaps inside porous materials and membranes [9–11]. Furthermore, the problem is related to the statistical mechanics of a quantum particle in a random potential [13], the behavior of flux lines in superconductors in the presence of columnar defects [14,15], and the problem of diffusion in a random catalytic environment [4].

In this paper we will study the static properties of a Gaussian polymer chain, without excluded volume interactions, that is confined in a quenched random medium. Experimentally, a polymer in a specific solvent is known to obey Gaussian statistics at the so called Θ temperature—where the long range self-avoiding interactions are effectively screened. The term quenched refers to the fact that the random medium is frozen and thus does not thermalize with the active degrees of freedom—in this case the polymer chain. We are interested in the properties of the polymer, such as the free energy and radius of gyration (or alternatively the end-to-end distance), that are averaged with the appropriate Wiener measure over all possible chain conformations in a given realization of the random medium, with a final average taken over all possible configurations of the random medium. The nature of the random environment is crucial in this problem, and so it is important to distinguish the following two important cases that have been discussed in the literature:

1. A Gaussian random potential with short range correlations.
2. Random obstacles which prevent the chain from visiting certain sites.

Numerical simulations performed in three dimensions were restricted, to our knowledge, only to the case of random obstacles [1,5,6]. Also, a numerical investigation based on the mapping to the Schrödinger equation in one dimension was performed for the Gaussian potential case [8]. On the other hand, extensive analytical work using the replica variational approach and Flory type free energy arguments, has been done for the case of a Gaussian random potential [2–4,7,8]. The case of a bounded (saturated) random potential was also addressed in [3]. It was not clear to us to what extent these theoretical investigations could be applied to the case of infinitely strong random obstacles placed randomly in the medium, as simulated numerically.

In this paper we investigate analytically, for the first time, the case of infinitely strong, randomly placed obstacles. We point out similarities and differences with the case of a Gaussian random potential, and also the case of a saturated potential. We will assume that the obstacles are infinitely strong—they totally exclude the chain from visiting a given site occupied by an obstacle. Each obstacle is taken to be a block of volume a^d , where d is the number of spatial dimensions and where a is the linear dimension of the block. We take for simplicity the polymer bond length b to be approximately equal to a . Thus, a will be the small length scale in the problem, and we will measure all distances in units of a . However, in the next section we will sometimes keep a explicitly in order to omit terms of higher order of smallness. The obstacles are placed on the sites of a cubic lattice with lattice spacing a .

^a e-mail: yadin@pitt.edu

We denote by x the probability that any given lattice site is occupied by an obstacle (block). Our main results will concern the case of small x , in particular $x < x_c$, where x_c refers to the percolation threshold ($x_c = 0.3116$ for a cubic lattice in $d = 3$), but we will also comment on the case of a larger concentration of obstacles. We denote by \mathcal{V} the total volume of the system.

For an uncorrelated Gaussian random potential, it was argued using qualitative arguments in references [3, 4] that a very long Gaussian chain will typically curl up in some small region of low average potential. The polymer chain is said to be localized, and for long chains the end-to-end distance (R_F) becomes independent of chain length and scales like

$$R_F \propto (g \ln \mathcal{V})^{-1/(4-d)}, \quad (1)$$

with g being the strength of the disorder (the random potential satisfies $\langle U(x)U(x') \rangle = g\delta(x - x')$). The depth of the well entrapping the chain is approximately

$$U_{\min} \sim -(g \ln \mathcal{V})^{2/(4-d)}. \quad (2)$$

These results were also obtained by the replica method in reference [7], and rederived using a mapping to a quantum particle's localization in reference [8]. For very short chains the end-to-end distance scales diffusively ($R_F^2 \sim L$), and it saturates at the R_F value quoted above for large L . Notice, that in the infinite volume limit, the chain completely collapses. This results from the fact that the depth of the potential is unbounded from below, and the chain is always able to find with reasonable probability a deep enough narrow potential well to occupy, overcoming its tendency to swell due to the entropy of confinement. The collapse of the chain in the infinite volume limit agrees with the results for a chain in an annealed potential, since the ability of a chain to scan all of space for a favorable environment is equivalent to the random potential adapting itself to the chain configuration.

To review briefly the argument leading to equations (1, 2) using localization theory [8] we recall that the density of states for a particle in an uncorrelated Gaussian random potential is given by [16]

$$\rho(E) = \frac{A}{|E|^\alpha} \exp(-B|E|^\delta), \quad (3)$$

with $\delta = (4-d)/2$ and $B \propto 1/g$, where g is the strength of the disorder. This result is valid for an infinite volume. In a finite volume \mathcal{V} the energy will be bounded from below. We can estimate the lowest energy E_c from the tail of the distribution:

$$\int_{-\infty}^{E_c} dE \rho(E) \simeq 1/\mathcal{V}, \quad (4)$$

which leads to

$$E_c = - \left(\frac{\ln \mathcal{V}}{B} \right)^{1/\delta}. \quad (5)$$

The width of the ground state wave function (localization length) is given by

$$\ell_c \sim |E_c|^{-1/2} \sim (g \ln \mathcal{V})^{-1/(2\delta)}. \quad (6)$$

The mapping from a quantum particle of mass m , at a finite temperature $1/\beta$, to a polymer chain, is given by

$$\hbar \rightarrow T, \quad \hbar\beta \rightarrow L, \quad m \rightarrow dT/b^2. \quad (7)$$

It can be shown that the ground state width ℓ_c is proportional to the end-to-end distance R_F of a chain that is situated in a deep minimum in the volume \mathcal{V} , whose depth is given by $E_c \sim U_{\min}$. Using the above mapping the density matrix for a quantum particle at finite temperature [17] corresponds to the partition sum (Green's function) of a Gaussian polymer chain [18].

2 Random obstacles

For the case of infinitely strong randomly placed obstacles, the potential energy of the polymer chain is always zero. Hence, the free energy of the polymer will be $F = -TS$, since $E = 0$, and the statistics of the polymer will be dictated only by entropic effects. As the volume of the system tends to infinity there is a chance to find very large lacunae free of obstacles. Thus, in the limit of large volume we do not expect the polymer to collapse, but rather to inflate with increasing number of monomers (L). We will now analyze the behavior of a polymer in an environment consisting of random obstacles and find that there are three different phases as a function of the volume of the system. In the subsequent analysis we will always assume that L is very large.

In order to estimate the average chain properties we first assume that a very long polymer chain will attain an approximately spherical shape of radius R (we will discuss this spherical droplet approximation in the sequel). Now, let us coarse grain the volume \mathcal{V} into subregions of volume $v \sim R^d$, and assume that the polymer is confined to one of these regions. Each of these coarse grained subregions will contain a different number of obstacles, and the chain will reside in that region with the lowest number of obstacles which can be found in the finite volume \mathcal{V} in order to minimize its free energy. We will estimate R by writing the free energy of the polymer as a function of both R and the coarse grained volume fraction of obstacles in a given subregion (which also depends on R), and minimizing it accordingly. First, let us assume that there are no obstacles present inside this spherical region. The entropy of a chain confined in this "cavity" is of the form

$$S = L \ln(z) - \alpha \frac{L}{R^2},$$

where z is the number of nearest neighbors, *e.g.* $2d$ for a cubic lattice in d dimensions, and the second term is the entropy of confinement [19]. Here, α is a numerical constant. The free energy will then be $F = -TS$. In the

following we choose $T = 1$ for simplicity since the temperature does not play any significant role with respect to the results.

In order to proceed and estimate the entropy change due to obstacles inside the volume v , we use the mapping from the polymer to a quantum particle as discussed in the introduction. The free energy per monomer of the polymer when L is very large corresponds to the ground state energy of a quantum particle in a cavity of radius R . This is known, in three dimensions, to be equal to $E_0 = (\hbar^2/2m)\pi^2/R^2$, in agreement with the expression above (up to an unimportant additive constant). In d dimensions the energy is still proportional to $1/R^2$ but the prefactor is different. Suppose that there is a spherical obstacle of radius a inside the sphere. If the obstacle is at the center of the sphere the Schrödinger equation is exactly solvable and the ground state in $d = 3$ is given by

$$\Psi(r) = C \frac{\sin \frac{\pi(r-R)}{R-a}}{r}, \quad a < r < R \quad (8)$$

and $\Psi(r) = 0$ otherwise. This will correspond to an energy of

$$\frac{m}{\hbar^2} E_0 = \frac{\pi^2}{2R^2} + \frac{\pi^2 a}{R^3} + \dots, \quad (9)$$

where the corrections vanish faster than a as $a \rightarrow 0$. If on the other hand the obstacle is not in the center of the sphere we could only find an approximate solution of the Schrödinger equation which can be used to give an upper bound to the ground state, which may be exact to leading order in a (see Appendix). The ground state energy becomes

$$\frac{m}{\hbar^2} E_0 = \frac{\pi^2}{2R^2} + \frac{\pi^2 a}{R^3} \left(\frac{R}{\pi R_0} \sin \frac{\pi R_0}{R} \right)^2 + \dots, \quad (10)$$

where R_0 is the distance of the center of the obstacle from the center of the sphere. One can see that the factor in parenthesis approaches 1 as $R_0 \rightarrow 0$, and vanishes as $R_0 \rightarrow R$. Notice, that for the analysis above we have treated the obstacles as spherical in shape as opposed to a square block. However, this difference should only amount to an unimportant numerical factor.

Using the mapping from the quantum particle to the polymer as given by equation (7), we find

$$\frac{m}{\hbar^2} E_0 \rightarrow \frac{3F}{a^2 L}, \quad (11)$$

where F is the free energy of the chain. We have used the fact that $T = 1$ and $b = a$ for the bond length. (This correspondence is up to an additive constant that is given by the entropy of a chain in free space.) Now, if the position of the obstacle is random we expect that we should average the energy over all the possible locations of the obstacle within the volume of the sphere to obtain

$$\frac{3F}{a^2 L} = \frac{\pi^2}{2R^2} + \frac{3a}{2R^3} + \dots \quad (12)$$

Let us denote by \hat{x} the volume fraction occupied by the random obstacles within the spherical volume v . Then the number of obstacles inside this volume will be $\frac{4\pi}{3}(R/a)^3 \hat{x}$. If \hat{x} is small the energy due to several obstacles will be approximately equal to the sum of the individual energies. The deviation from this rule becomes important only if the obstacles are very close or touching each other, and for small \hat{x} the number of such configurations is very small compared with configurations where the obstacles don't touch. In any case interactions among obstacles are at least of $O(\hat{x}^2)$. Thus, the free energy of a polymer chain confined to a volume v , with a volume fraction \hat{x} occupied by obstacles, is

$$\frac{F}{L} = \frac{\pi^2}{6(R/a)^2} + \frac{2\pi}{3} \hat{x} + \dots \quad (13)$$

The important conclusion is that the term proportional to \hat{x} is independent of R . The numerical prefactors are really of no importance to us. The small \hat{x} approximation is enhanced by the fact that not only do we assume that x is small ($x < x_c$), but the chain will be found to settle in regions where the obstacle concentration is smaller than average. In two dimensions we find that the first term in equation (12) is proportional to $1/R^2$ and the second term to $1/(R^2 |\ln(a/R)|)$ (see Appendix). In one dimension the situation is totally different since an obstacle will divide the volume v into two disjoint regions. Thus, all our conclusions apply only above two dimensions, where the second term in equation (12) is proportional to $a^{d-2} R^{-d}$. When multiplying by the number of obstacles $\sim (R/a)^d \hat{x}$ one gets an R -independent result for the second term in equation (13). Two dimensions is a borderline case where some subtleties may arise. In the following we will measure all distances in units of a so we put $a = 1$.

We now proceed to study the chain statistics by considering the fluctuations of the volume fraction \hat{x} . If x is the probability that a lattice site is occupied by an obstacle, then the coarse grained volume fraction \hat{x} is distributed according to the binomial probability distribution $b(v\hat{x}; v, x)$. The notation

$$b(k; n, p) = \binom{n}{k} p^k q^{n-k}, \quad (14)$$

stands for the probability that n Bernoulli trials with probabilities p for success and $q = 1 - p$ for failure result in k successes and $n - k$ failures [20]. For $\hat{x} = 0$ it gives the so called Lifshits probability to find an empty region of volume v free of obstacles. With this probability there will be associated an "entropy" which will be its logarithm.

Using the results above we can start to discuss the statistics of a polymer in an infinite volume ($V \rightarrow \infty$)—the so called annealed result. Assuming that the chain takes on a roughly spherical configuration of volume $v \sim R^d$, the free energy will read

$$F(R, \hat{x}) = -L \ln(z) + \frac{L}{R^2} + L\hat{x} - \ln [b(R^d \hat{x}; R^d, x)]. \quad (15)$$

This free energy has to be minimized both with respect to \hat{x} , and to R , since the chain is free to move and find the most favorable values for these parameters. The most favorable value of \hat{x} for large L and for an infinite volume is $\hat{x} = 0$, since \hat{x} is not allowed to be negative. Using the fact that

$$b(0; v, x) = (1 - x)^v, \quad (16)$$

we find that the expression for the free energy becomes

$$F(R) = -L \ln(z) + \frac{L}{R^2} - R^d \ln(1 - x). \quad (17)$$

This free energy has now to be minimized with respect to R to yield

$$R_{\text{m,annealed}} \sim \left(\frac{L}{|\ln(1 - x)|} \right)^{1/(d+2)}. \quad (18)$$

Thus the size of the chain grows with L , but with an exponent smaller than $1/2$, the free chain exponent.

So far we discussed the case of an infinite volume \mathcal{V} . In a finite volume we find that the so called quenched and annealed case differ, at least when the volume is not too big. We actually find that there are three regions as a function of the size of the system volume \mathcal{V} . First, if $\mathcal{V} < \mathcal{V}_1 \simeq \exp(x^{-(d-2)/2}/(1-x))$, it is unlikely for a chain of volume $v \sim R^d$ to find a region which is totally free of obstacles. Thus \hat{x} does not vanish in this regime. To proceed further we must use an approximation to the binomial distribution $b(v\hat{x}; v, x)$.

If v is not too small we can approximate the binomial distribution by a normal distribution [20]

$$b(v\hat{x}; v, x) \approx (2\pi vx(1-x))^{-1/2} \times \exp\left(-\frac{v(\hat{x}-x)^2}{2x(1-x)}\right). \quad (19)$$

This approximation is good provided $vx \gg 1$ and $v(1-x) \gg 1$. We will verify below that these conditions are indeed met in our case when x is small.

In a finite volume \mathcal{V} , the lowest expected value of \hat{x} , to be denoted by \hat{x}_{m} , can be found from the tail of the distribution

$$\int_0^{\hat{x}_{\text{m}}} d\hat{x} \exp\left(-\frac{v(\hat{x}-x)^2}{2xy}\right) \simeq \frac{v}{\mathcal{V}}, \quad (20)$$

which gives

$$\hat{x}_{\text{m}} \simeq x - \sqrt{\frac{xy \ln \mathcal{V}}{R^d}}. \quad (21)$$

The free energy becomes

$$F_1(R) = -L \ln(z) + \frac{L}{R^2} + Lx - L\sqrt{\frac{xy \ln \mathcal{V}}{R^d}}. \quad (22)$$

The last term in equation (15) is missing since it is negligible for large L when R is independent of L . Minimizing $F(R)$ with respect to R we find

$$R_{\text{mI}} \sim (xy \ln \mathcal{V})^{-1/(4-d)} \quad (23)$$

and

$$\hat{x}_{\text{mI}} = x - (xy \ln \mathcal{V})^{2/(4-d)}, \quad (24)$$

where we put $y = 1 - x$. The result for the radius of gyration of the chain, as represented by R_{mI} is the same result as for the case of the Gaussian distributed random potential, but with the strength g replaced by $x(1-x)$. The polymer in this case is localized and its size is independent of L for large L .

As \mathcal{V} grows R_{m} decreases until eventually \hat{x}_{m} vanishes. This happens when $\mathcal{V} = \mathcal{V}_1 \simeq \exp(x^{-(d-2)/2}y^{-1})$. For $\mathcal{V} > \mathcal{V}_1$, R_{m} is no longer given by equation (23), but rather by the solution of $\hat{x}_{\text{mII}} = 0$. It is the largest region free of obstacles expected to be found in a volume \mathcal{V} . Rather than using the normal approximation we can estimate R_{m} directly from the relation

$$(1-x)^v \simeq v/\mathcal{V}, \quad (25)$$

with $v \sim R_{\text{m}}^d$. Solving for R_{m} we obtain

$$R_{\text{mII}} \sim \left(\frac{\ln \mathcal{V}}{|\ln(1-x)|} \right)^{1/d}. \quad (26)$$

The polymer is still localized but the dependence on x and on $\ln \mathcal{V}$ has changed. In this region which we call region II the free energy is given by

$$F_{\text{II}} = -L \ln(z) + \alpha L \left(\frac{\ln \mathcal{V}}{|\ln(1-x)|} \right)^{-2/d}, \quad (27)$$

where some undetermined constant α is introduced for later convenience.

As \mathcal{V} grows in region II, R_{mII} continues to grow until it reaches the annealed value given in equation (18). This happens when

$$\mathcal{V} = \mathcal{V}_2 \sim \exp\left(x^{2/(d+2)}L^{d/(d+2)}\right) \quad (28)$$

to leading order in x , which is enormous for large L . For $\mathcal{V} > \mathcal{V}_2$ we have the third region in which $R_{\text{mIII}} = R_{\text{m,annealed}}$ and it grows like $L^{1/(d+2)}$.

Since in region I we have used the normal approximation to the binomial distribution, we should check *a posteriori* if the condition $vx \gg 1$ is met. Since $\mathcal{V} < \mathcal{V}_1$ we find

$$C_d R_{\text{mI}}^d x \approx C_d x^{-(d-2)/2} \left(\frac{\ln \mathcal{V}_1}{\ln \mathcal{V}} \right)^{d/(4-d)} > C_d x^{-(d-2)/2}. \quad (29)$$

Here $C_d = 2\pi^{d/2}/(d\Gamma(d/2))$ is the volume of a d -dimensional sphere of unit radius. In $d = 3$, for example, $C_3 = 4\pi/3$. Thus we see that for $d > 2$, $vx \gg 1$ provided $x \ll 1$. The minimum value is attained for $\mathcal{V} = \mathcal{V}_1$, and is significantly larger when $\mathcal{V} < \mathcal{V}_1$. It is interesting to notice that in $d = 3$ for example, even if $x = 0.3$, we find that $C_3/\sqrt{x} = 7.6$ which is considered large enough for

the validity of the normal approximation (a value of 5 is usually considered sufficient).

Actually, the normal approximation to the binomial distribution $b(k; n, p)$ is not entirely accurate even if the conditions $np \gg 1$ and $nq \gg 1$ are met, if k is far from the center, *i.e.* if $|k - np|^3/n^2 > 1$ [20]. In our case we need that $v|\hat{x}_m - x|^3 < 1$ to be satisfied. In region I we have

$$C_d R_{mI}^d |\hat{x}_{mI} - x|^3 < C_d (xy \ln \mathcal{V}_1)^{(6-d)/(4-d)} = C_d x^{(6-d)/2}, \quad (30)$$

where we have used equation (24) and the value of \mathcal{V}_1 . For $d = 3$ this is smaller than one even for $x = 0.3$.

The behavior in region II can also be deduced from known results of the density of states for a quantum particle in the presence of obstacles (repulsive impurities). In that case [16] the density of states is given by (when the obstacles are placed on a lattice)

$$\rho(E) \sim \exp(-c|\ln(1-x)|E^{-d/2}), \quad E > 0 \quad (31)$$

with c being some dimension dependent constant and x is the density of impurities. Note that $\rho(E)$ vanishes for $E < 0$. We can estimate the lowest energy in a finite volume \mathcal{V} from the integral

$$\int_0^{E_c} dE \rho(E) \simeq 1/\mathcal{V}, \quad (32)$$

and find

$$E_c \sim \left(\frac{\ln \mathcal{V}}{|\ln(1-x)|} \right)^{-2/d}, \quad (33)$$

and thus the localization length is given by

$$\ell_c \sim |E_c|^{-1/2} \sim \left(\frac{\ln \mathcal{V}}{|\ln(1-x)|} \right)^{1/d}, \quad (34)$$

which coincides with R_{mII} above.

To conclude this section we make some remarks on the validity of the spherical droplet approximation. The shape of a long polymer chain is determined by the regions of the random medium that have a lower than average number of obstacles. For $\mathcal{V} > \mathcal{V}_1$ these regions are essentially free of obstacles. The probability of finding such empty regions depends only on its volume and not its shape. However given regions of varying shapes and equal volumes, it will be entropically more favorable for a long polymer chain to reside in a region whose shape is closest to a sphere. This is because the confinement entropy is maximized for a sphere over other shapes of the same volume. The argument is equivalent to that proposed by Lifshits [16] in the context of electron localization and is shown rigorously by Luttinger [21]. For $\mathcal{V} > \mathcal{V}_1$ the relevant regions contain a small number of obstacles but we believe that the same argument should roughly hold and deviations from a spherical shape will be small or irrelevant.

3 Comparison with numerical simulations

We have compared our results from the last section with numerical simulations performed by Dayantis *et al.* [6], and also comment on the relation to earlier simulations done by Baumgartner and Muthukumar [1]. Dayantis *et al.* carried out simulations of free chains (random-flight walks) confined to cubes of various linear dimensions 6 – 20, in units of the lattice constant. These chains can intersect freely and lie on a cubic lattice. They introduced random obstacles with concentrations $x = 0, 0.1, 0.2$ and 0.3. The length of the chains vary between 18 – 98 steps. They also simulated self-avoiding chains that we will not discuss here. They measured the quenched entropy, the end-to-end distance, and also the radius of gyration which is a closely related quantity. Unfortunately, these authors did not have a theoretical framework to analyze their data, and thus could not make it collapse in any meaningful way. We show below how it is possible to fit the data nicely to our analytical results.

Even for $x = 0.1$, the value that we get for \mathcal{V}_1 is about 33 which is an order of magnitude smaller than the smallest volume used in their simulation, which is 216 for a cube of side 6. Hence we expect to be in region II. To check the agreement with our analytical results we show in Figure 1 a plot of $\ln(-S/L + \ln 6)$ *vs.* $\ln(\ln \mathcal{V}/|\ln(1-x)|)$ where S is the entropy measured in the simulations and $\mathcal{V} = B^3$ for a box of side B . Recall that $F = -S$ and equation (27) predicts a straight line with slope $-2/3$. The best fit is obtained for a slope of -0.72 ± 0.05 , which is in excellent agreement with our analytical results in region II.

In order to analyze the simulation results for the end-to-end distance and radius of gyration we have to introduce some additional compensation for the results obtained in the previous section. First we must realize that equation (26) is valid only when the number of steps (monomers) is very large. In the simulations they used chains of varying lengths whose size did not yet reach asymptotia. Hence, we introduce a correction factor

$$R_m(L) = R_m(1 - \exp(-L/R_m^2))^{1/2} \equiv R_m f_1(\sqrt{L}/R_m), \quad (35)$$

which interpolates between the size of a free chain as $L \rightarrow 0$ and the value of R_m from equation (26) as $L \rightarrow \infty$.

The second correction we have to implement arises when the expected value of the chain is not much smaller than the size of the confining box. Even for a free chain confined to a box of side B with no obstacles present, the end-to-end distance is not simply $R = L^{1/2}$ for $L^{1/2} < B$ and $R = B$ for larger L . We have to take into account the fact that the length of the chain has a Gaussian distribution about its expected value, and the tail of the Gaussian is cut off by the presence of the box (this is for the absorbing boundary conditions that is used in the simulations). Thus, for the case of no obstacles ($x = 0$), The measured

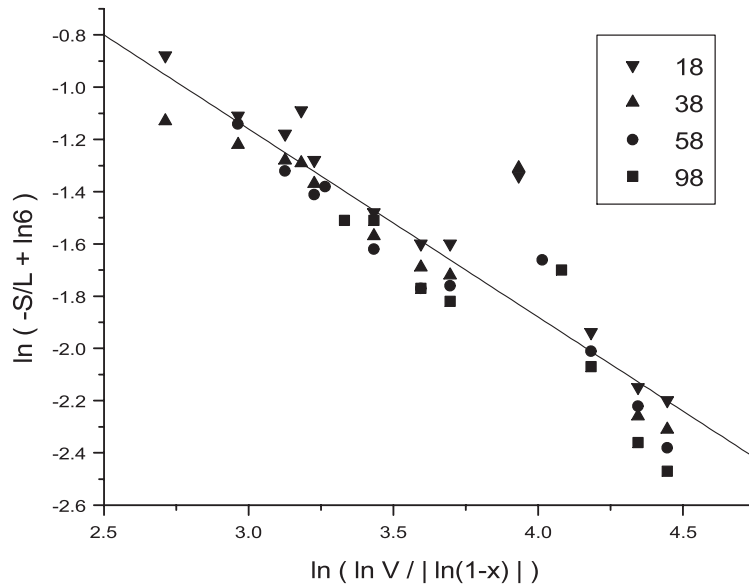


Fig. 1. A plot of $\ln(-S/L + \ln 6)$ vs. $\ln(\ln V / |\ln(1-x)|)$. The labels are marked according to the chain length.

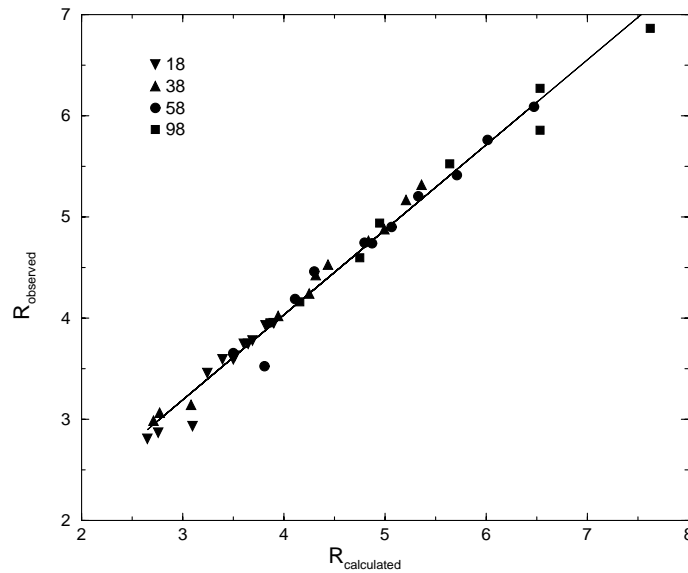


Fig. 2. A plot of the observed vs. calculated end-to-end distance.

end-to-end distance should approximately be

$$R_c^2 = \int_{-B}^B dR R^2 \exp\left(-\frac{R^2}{2L}\right) \bigg/ \int_{-B}^B dR \exp\left(-\frac{R^2}{2L}\right), \quad (36)$$

which gives $R_c = \sqrt{L} f_2(B/\sqrt{L})$ with

$$f_2(x) = \left(1 - \sqrt{\frac{2}{\pi}} \frac{x}{\operatorname{erf}(x/\sqrt{2})} \exp(-x^2/2)\right)^{1/2}. \quad (37)$$

This indeed gives good agreement with the measured values in the no obstacle case. For the obstacle case we thus have to introduce these two corrections in subsequent

order:

$$R_{m,\text{corrected}} = R_m f_1(\sqrt{L}/R_m) f_2\left(\frac{B}{R_m f_1(\sqrt{L}/R_m)}\right), \quad (38)$$

where $R_m = R_{mII}$ as given by equation (26). (A constant of proportionality of 1.8 has been introduced on the rhs of equation (26) to obtain a good fit). In Figures 2 and 3 we show a comparison of the simulation results for the end-to-end distance and for the radius of gyration with the calculated results as given by equations (26, 38). The agreement seems remarkable, especially for the end-to-end distance, where all the data collapses to a straight line with a slope close to 1.

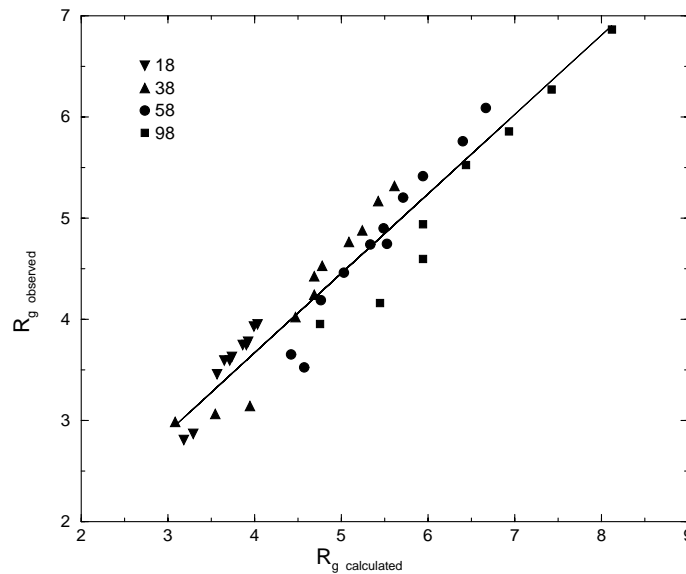


Fig. 3. A plot of the observed *vs.* calculated radius of gyration.

Dayantis *et al.* emphasize that they did not consider concentrations of obstacles above the percolation threshold, which is at $x_c = 0.3116$ for a simple cubic lattice. The reason is that above the percolation threshold the medium of random obstacles begins to form disconnected islands free of obstacles. Thus, in their simulation the polymer chain will only sample a limited fraction of the volume available. What happens is that effectively the volume available for the chain is not the total volume of the cube but rather the volume of the disconnected region it occupies. For most realizations of the random medium this effective volume will be smaller than the value \mathcal{V}_1 , which is the limit of region I of the last section. In that case one expects the end-to-end distance to scale like x^{-1} as given in equation (23) instead of like $x^{-1/3}$ as given by equation (26). Baumgartner and Muthukumar's simulation was for both below the percolation threshold and also above it ($x = 0.4$ and 0.5). However, they only estimate the exponent above the percolation threshold, and find it to be about -1 . They do not estimate the exponent for x below the percolation threshold, which appears from their data to scale with a much smaller exponent. Thus, it seems likely that the reason these authors report a behavior corresponding to region I, even though their box is quite large, is because the effective volume is small for the cases for which they exceed the percolation threshold.

4 Summary and discussion

In this paper we have considered the effect of random obstacles on the behavior of a free Gaussian chain. We have seen that in the presence of infinitely strong obstacles, that exclude the chain from visiting randomly chosen sites, there are three possible behaviors of the end-to-end distance as a function of L (the number of monomers). The three possible regimes depend on the total volume of the system. If the volume of the system is smaller

than $\mathcal{V}_1 \simeq \exp(x^{-(d-2)/2})$, where x is the probability that a lattice site is occupied, then the polymer is localized, as in the case of a Gaussian random potential, and $R_I \sim (x \ln \mathcal{V})^{-1/(4-d)}$. For $\mathcal{V}_1 < \mathcal{V} < \mathcal{V}_2$, where $\mathcal{V}_2 \sim \exp(x^{2/(d+2)} L^{d/(d+2)})$, the polymer size is given by $R_{II} \sim (x/\ln \mathcal{V})^{-1/d}$. Finally, for $\mathcal{V} > \mathcal{V}_2$, the polymer behaves the same way as for an annealed potential, *i.e.* $R_{III} \sim (L/x)^{1/(d+2)}$. We have displayed the results to leading order in x for small x . These results are valid only when the average volume fraction of the obstacles (x) is smaller than the percolation threshold. When x is bigger than the percolation threshold we expect that the system breaks into independent domains whose volume is independent of, and generally much smaller than, the total volume of the system.

We were able to fit nicely the simulations of Dayantis *et al.* [6] to the analytic behavior in region II. The results of Baumgartner and Muthukumar for $x > x_c$, presumably correspond to region I. Region III is very difficult to be seen in simulations since \mathcal{V}_2 is huge for large L . However such behavior, which coincides with the annealed case have been obtained by Chandler *et al.* [5] in their simulations of annealed random obstacles.

The behavior in the three regions has some similarities to the case of a saturated random potential as discussed by Cates and Ball [3]. However, there are also significant differences. The saturated potential discussed by these authors concerned the case where the random potential can take two different values $\pm\sqrt{g}$ with probability $1/2$ each. They considered the case when g is small. In that case, when the chain occupies an approximately spherical volume R^d , its energy is estimated by the average potential in that region times the number of monomers L of the chain. This leads to a coarse grained renormalized potential with a Gaussian probability distribution that is valid provided the predicted size of the chain is much larger than the largest cavity that is free of obstacles. On the other hand,

in the case of infinitely strong obstacles the free energy of a chain occupying a volume R^d has a completely entropic origin. The energy of the chain remains zero as it is completely excluded from the regions occupied by obstacles. In the case of a saturated potential the behavior in region I is given by $R_{\text{SI}} \sim (g \ln \mathcal{V})^{-1/(4-d)}$, so in this region g plays a similar role to x (the subscript S refers to the saturated potential case). However, the volume of the system beyond which this behavior is no longer valid is given by $\mathcal{V}_{\text{SI}} \simeq \exp(g^{-d/4})$, which is quite different from its value in the strong obstacle case. Here $d = 2$ is no longer a lower critical dimension, and the result, which has a very different d -dependence, is valid down to (and including) one dimension. For $\mathcal{V}_{\text{SI}} < \mathcal{V} < \mathcal{V}_{\text{S2}}$, one has $R_{\text{SII}} \sim (\ln \mathcal{V})^{1/d}$, independent of g . Also $\mathcal{V}_{\text{S2}} \sim \exp(L^{d/(d+2)})$, independent of g . Above \mathcal{V}_{S2} the annealed result $R_{\text{SIII}} \sim L^{1/(d+2)}$ applies.

As compared to the unsaturated Gaussian random potential, the two models coincide only in region I when $\mathcal{V} < \mathcal{V}_1$. For $\mathcal{V} \rightarrow \infty$ the polymer collapses to a point in the Gaussian potential case as it can find a very deep and narrow potential well, whereas in the random obstacle case the polymer swells as $L^{1/(d+2)}$ with growing L as it can find large lacunae free of obstacles. Our analysis of the simulations of Dayantis *et al.* [6] shows clearly that their results do not conform to the behavior dictated by the Gaussian random potential model but are described well by the expected behavior in the intermediate region II.

This research is supported by the US Department of Energy (DOE), grant No. DE-FG02-98ER45686.

Appendix

Consider a spherical cavity of radius R about the origin. Inside the cavity there is one obstacle of radius a , centered at location \mathbf{R}_0 . The potential within the obstacle is infinite and thus the wave function has to vanish in that region. We will assume that $a \ll R$. Let us define the unperturbed wave function

$$\Psi_0(\mathbf{r}) = \frac{A}{|\mathbf{r}|} \sin \frac{\pi|\mathbf{r}|}{R}. \quad (\text{A.1})$$

This is the ground state solution of the Schrödinger equation in the absence of the obstacle.

Consider now the following trial wave function:

$$\Psi(\mathbf{r}) = \begin{cases} 0, & 0 < |\mathbf{r} - \mathbf{R}_0| < a \\ \Psi_0(\mathbf{r})\Psi_1(\mathbf{r} - \mathbf{R}_0), & a < |\mathbf{r} - \mathbf{R}_0| < r_m \\ \Psi_0(\mathbf{r}), & r_m < |\mathbf{r} - \mathbf{R}_0| \quad \&\& \quad |\mathbf{r}| < R \end{cases} \quad (\text{A.2})$$

with

$$\Psi_1(\mathbf{r}) = \frac{r_m}{\sin\left(\frac{\pi(r_m - a)}{R}\right)} \frac{1}{|\mathbf{r}|} \sin\left(\frac{\pi(|\mathbf{r}| - a)}{R}\right). \quad (\text{A.3})$$

Here r_m is determined by the condition

$$\nabla\Psi_1(\mathbf{r})|_{|\mathbf{r}|=r_m} = 0, \quad (\text{A.4})$$

which leads to the condition

$$\tan\left(\frac{\pi(r_m - a)}{R}\right) = \frac{\pi r_m}{R}. \quad (\text{A.5})$$

In the limit of small a this leads to

$$r_m \simeq \left(\frac{3}{\pi^2}\right)^{1/3} R^{2/3} a^{1/3}. \quad (\text{A.6})$$

Thus the volume of the region around the obstacle in which the wave function deviates from Ψ_0 is about $4R^2 a/\pi$, which vanishes like a as $a \rightarrow 0$, not like a^3 . In the following we will refer to this volume as V_a . The choice of r_m is designed to insure that not only the wave function but also its gradient are continuous across the seam $|\mathbf{r} - \mathbf{R}_0| = r_m$. Thus As $|\mathbf{r} - \mathbf{R}_0| \rightarrow r_m$ from below

$$\nabla\Psi = \Psi_1\nabla\Psi_0 + \Psi_0\nabla\Psi_1 \rightarrow \nabla\Psi_0, \quad (\text{A.7})$$

since $\nabla\Psi_1 \rightarrow 0$ and $\Psi_1 \rightarrow 1$.

Using this wave function an upper bound on the energy is given by

$$\frac{m}{\hbar^2} E_0 \leq \frac{\int \Psi(\mathbf{r})(-\frac{1}{2}\nabla^2)\Psi(\mathbf{r})dV}{\int \Psi^2(\mathbf{r})dV}. \quad (\text{A.8})$$

Evaluating the rhs we find

$$\frac{m}{\hbar^2} E_0 \leq \frac{\pi^2}{2R^2} + \frac{\int \Psi(\mathbf{r})(-\frac{1}{2}\nabla^2 - \frac{\pi^2}{2R^2})\Psi(\mathbf{r})dV_a}{\int \Psi_0^2(\mathbf{r})dV} + O(a^2), \quad (\text{A.9})$$

where in the numerator we only integrate over the volume V_a about the obstacle. Now, inside V_a

$$\nabla^2\Psi(\mathbf{r}) = \Psi_1(\mathbf{r} - \mathbf{R}_0)\nabla^2\Psi_0(\mathbf{r}) + \Psi_0(\mathbf{r})\nabla^2\Psi_1(\mathbf{r} - \mathbf{R}_0) + \nabla\Psi_0(\mathbf{r}) \cdot \nabla\Psi_1(\mathbf{r} - \mathbf{R}_0). \quad (\text{A.10})$$

We argue that

$$\int dV_a \nabla\Psi_0(\mathbf{r}) \cdot \nabla\Psi_1(\mathbf{r} - \mathbf{R}_0),$$

vanishes faster than a in the limit $a \rightarrow 0$, because of the angular integration: $\nabla\Psi_0(\mathbf{r})$ points in a fixed direction away from the origin at $\mathbf{0}$, whereas $\nabla\Psi_1(\mathbf{r} - \mathbf{R}_0)$ points in a varying radial direction away from the center at \mathbf{R}_0 , and thus the angular integration will yield $\int_{-1}^1 \cos\theta d\cos\theta = 0$. We have actually verified that the contribution of this term is $O(a^{5/3})$, hence negligible. Since $-(1/2)\nabla^2\Psi_0(\mathbf{r}) = (\pi^2/2R^2)\Psi_0(\mathbf{r})$, the first term in equation (A.10) exactly cancels the second term of the integral in the numerator of equation (A.9). Thus we are left with

$$\frac{m}{\hbar^2} E_0 \leq \frac{\pi^2}{2R^2} + \frac{\int \Psi_0^2(\mathbf{r})\Psi_1(\mathbf{r} - \mathbf{R}_0)(-\frac{1}{2}\nabla^2)\Psi_1(\mathbf{r} - \mathbf{R}_0)dV_a}{\int \Psi_0^2(\mathbf{r})dV}. \quad (\text{A.11})$$

At this point we can approximate $\Psi_0^2(\mathbf{r})$ by its value at $\mathbf{r} = \mathbf{R}_0$, and take it out of the integral. Also,

$$\left(-\frac{1}{2}\nabla^2\right)\Psi_1(\mathbf{r}-\mathbf{R}_0) = (\pi^2/2R^2)\Psi_1(\mathbf{r}-\mathbf{R}_0).$$

Thus

$$\frac{m}{\hbar^2}E_0 \leq \frac{\pi^2}{2R^2} + \frac{\pi^2}{2R^2}\Psi_0^2(\mathbf{R}_0)\frac{\int\Psi_1^2(\mathbf{r})dV_a}{\int\Psi_0^2(\mathbf{r})dV}. \quad (\text{A.12})$$

Evaluating the integrals and using the estimate for r_m as given by equation (A.6), we arrive at the final result

$$\frac{m}{\hbar^2}E_0 = \frac{\pi^2}{2R^2} + \frac{\pi^2 a}{R^3}\left(\frac{R}{\pi R_0}\sin\frac{\pi R_0}{R}\right)^2 + \dots, \quad (\text{A.13})$$

as given in Section 2, where R_0 is the magnitude of \mathbf{R}_0 . Although we have used an approximate wave function that can give only an upper bound on the correction, it appears likely that the correction might be exact to leading order in a . Support for this comes from the fact that it coincides with the exact answer in the limit $R_0 = 0$.

We now consider briefly the two dimensional case. In this case we consider only the case where the obstacle is in the middle of the circular region. Without the obstacle present, the ground state solution to the Schrödinger equation is given by

$$\Psi_0(\mathbf{r}) = AJ_0\left(\frac{2.405r}{R}\right), \quad (\text{A.14})$$

where J_0 is the spherical Bessel function and $x_0 \simeq 2.405$ is its first zero. This leads to

$$\frac{m}{\hbar^2}E_0 = \frac{1}{2}\frac{x_0^2}{R^2}. \quad (\text{A.15})$$

With an obstacle of radius r present at the center, we look for a wave function of the form

$$\Psi_0(\mathbf{r}) = \begin{cases} AJ_0(kr) + BN_0(kr), & r > a \\ 0, & r < a \end{cases} \quad (\text{A.16})$$

where N_0 is Neumann's function, sometimes denoted by Y_0 . The variable k is determined by the requirement that $\Psi_0(r) = 0$ at $r = a$ and $r = R$. This leads to the condition

$$\frac{J_0(kR)}{N_0(kR)} = \frac{J_0(ka)}{N_0(ka)}. \quad (\text{A.17})$$

Thus

$$\frac{J_0(kR)}{N_0(kR)} \approx \frac{1 + O(k^2a^2)}{(2/\pi)(\ln(ka) + \gamma - \ln 2) + O(k^2a^2)}, \quad (\text{A.18})$$

and we find

$$k \approx \frac{x_0}{R} + \frac{\alpha}{R|\ln\frac{a}{R}|}, \quad (\text{A.19})$$

with

$$\alpha = \frac{\pi N_0(x_0)}{2 J_0'(x_0)}. \quad (\text{A.20})$$

Here J_0' is the derivative of J_0 with respect to its argument. It thus follows that

$$\frac{m}{\hbar^2}E_0 \approx \frac{1}{2}\frac{x_0^2}{R^2} + \frac{x_0\alpha}{R^2|\ln\frac{a}{R}|}. \quad (\text{A.21})$$

References

1. A. Baumgartner, M. Muthukumar, J. Chem. Phys. **87**, 3082 (1987); see also review chapter by these authors in Adv. Chem. Phys. (Vol. XCIV), *Polymeric Systems*, edited by I. Prigogine, S.A. Rice (John Wiley & Sons, Inc., New York, 1996) and references therein.
2. S.F. Edwards, M. Muthukumar, J. Chem. Phys. **89**, 2435 (1988).
3. M.E. Cates, R.C. Ball, J. Phys. France **49**, 2435 (1988).
4. T. Nattermann, W. Renz, Phys. Rev. A **40**, 4675 (1989).
5. K. Leung, D. Chandler, J. Chem. Phys. **102** (3), 1405, (1995); D. Wu, K. Hui, D. Chandler, J. Chem. Phys. **96** (1), 835, (1992).
6. J. Dayantis, M.J.M. Abadie, M.R.L. Abadie, Comput. Theoret. Polymer Sci. **8**, 273 (1998).
7. Y.Y. Goldschmidt, Phys. Rev. E **61**, 1729 (2000).
8. Y. Shiferaw, Y.Y. Goldschmidt, Phys. Rev. E **63**, 051803 (2001).
9. D.S. Cannell, F. Rondelez, Macromolecules **13**, 1599 (1980).
10. G. Guillot, L. Leger, F. Rondelez, Macromolecules **18**, 2531 (1985).
11. M.T. Bishop, K.H. Langley, F. Karasz, Phys. Rev. Lett. **57**, 1741 (1986).
12. L. Liu, P. Li, S.A. Asher, Nature (London) **397**, 141 (1999); L. Liu, P. Li, S.A. Asher, J. Am. Chem. Soc. **121**, 4040 (1999).
13. Y.Y. Goldschmidt, Phys. Rev. E **53**, 343 (1996).
14. D.R. Nelson, V.M. Vinokur, Phys. Rev. B **48**, 13060 (1993).
15. Y.Y. Goldschmidt, Phys. Rev. B **56**, 2800 (1997).
16. I.M. Lifshits, S.A. Gredeskul, L.A. Patur, *Introduction to the Theory of Disordered Systems* (Wiley, NY, 1988); I.M. Lifshits, Adv. Phys. **13**, 483 (1964).
17. R.P. Feynman, *Statistical Mechanics: A Set of Lectures* (Benjamin, New York, 1972).
18. M. Doi, S.F. Edwards, *The Theory of Polymer Dynamics* (Oxford University Press, Oxford, 1986).
19. P.G. de Gennes, *Scaling Concepts in Polymer Physics* (Cornell Univ. Press, Ithaca, 1979).
20. W. Feller, *An Introduction to Probability and its Applications* (Wiley, New York, 1963).
21. J.M. Luttinger in, *Path Integrals and their Applications in Quantum, Statistical, and Solid State Physics*, edited by G.J. Papadopoulos, J.T. Devreese (Plenum Press, New York, 1978).